Journal of Thermal Analysis and Calorimetry, Vol. 62 (2000) 729–736

SPECTROSCOPIC, MAGNETIC AND THERMAL INVESTIGATIONS ON Cu(II), Mn(II), Co(II) AND Fe(III) COMPLEXES WITH GLUTAMYL NITROANILIDE

L. Ghizdavu[1]*, C. Bălan*[2]*, L. David*[2]*, C. Bâtiu*[1]*, O. Cozar*[2] *and D. Ristoiu*[2]

[1]Department of Chemistry 'Babeş-Bolyai' University, 3400 Cluj-Napoca
[2]Department of Physics, 'Babeş-Bolyai' University, 3400 Cluj-Napoca, Romania

(Received November 19, 1999; in revised form March 27, 2000)

Abstract

New complexes $CuL_2{\cdot}2H_2O$, $CoL_2{\cdot}3H_2O$, $MnL_2{\cdot}2H_2O$ and $FeL_3{\cdot}2H_2O$, L=γ-*L*-glutamyl-5-(*p*-nitroanilide), were synthesized and characterized by their spectral, magnetic and thermal properties. The thermal stabilities of the synthesized complexes were examined in the temperature range 20–500°C. In all these complexes γ-*L*-glutamyl-5-(*p*-nitroanilide) acts as a bidentate ligand, its coordination involving the carbonyl oxygen and the nitrogen atom of the second amino group. The local structure around the Cu(II) ion is pseudotetrahedral. In the Co(II), Mn(II) and Fe(III) complexes, the metal ions are in the high-spin form, with octahedral stereochemistry.

Keywords: ESR spectroscopy, γ-*L*-glutamyl-5-(*p*-nitroanilide), IR spectroscopy, metal complexes

Introduction

Glutamic acid is widely used in protein chemistry, especially for the synthesis of simple peptides of physiological importance, e.g. glutathione. α- and β-glutamyl amides are a class of compounds with proved biological activity; they have been tested as anti-inflammatory, antitumoral, immunostimulatory, analgesic and diagnosis reagents [1–8]. The diagnosis of some pancreatic and liver diseases are based on determination of the activity of γ-glutamyltransferase (γ-GT). γ-*L*-Glutamyl-5-(*p*-nitroanilide) has been successfully used as a biochemical reagent. γ-GT binds to the substrate, breaks the amide bonding and transfers the glutamyl radical to the amino group of an N-terminal peptide (e.g. glycyl-glycine), releasing *p*-nitroaniline, which

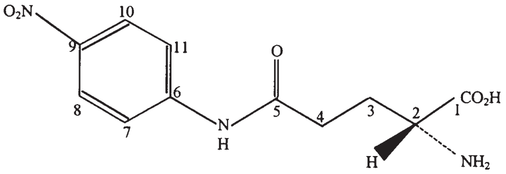

Fig. 1 The ligand γ-*L*-glutamyl-5-(*p*-nitroanilide)

1418–2874/2000/ $ 5.00

Akadémiai Kiadó, Budapest
Kluwer Academic Publishers, Dordrecht

can be detected spectrophotometrically. γ-*L*-Glutamyl-5-(*p*-nitroanilide) has also proved to be a useful inhibitor of the urease in the soil [9].

Given the important biochemical applications of γ-*L*-glutamyl-5-(*p*-nitroanilide) (Fig. 1), this paper presents an account of the synthesis and some chemical-physical properties of its transition metal complexes with *M*=Cu(II), Co(II), Mn(II) and Fe(III).

Experimental

The metal complexes were synthesized by the following procedure. Solutions of $CuSO_4\cdot 5H_2O$, $CoSO_4\cdot 7H_2O$, $MnSO_4\cdot 7H_2O$ and $Fe(NH_4)(SO_4)_2\cdot 12H_2O$ in distilled water were mixed with ligand dissolved in NaOH solution (pH=9). The precipitates formed were filtered off, washed with NaOH solution (pH=9) and then with water, dried and kept in dark-coloured bottles.

Some chemical-physical properties of the synthesized metal complexes are given in Table 1. The complexes are slightly soluble in water, insoluble in non-polar organic solvents (diethyl ether, $CHCl_3$, CCl_4, benzene and toluene) and soluble in some polar organic solvents (acetone, DMFA and DMSO). The complexes decompose in boiling organic solvents (colour change, turbulence, etc.).

Table 1 Some physical and elemental analytical data on the synthesized metal compounds

		$CuL_2\cdot 2H_2O$	$CoL_2\cdot 3H_2O$	$MnL_2\cdot 2H_2O$	$FeL_3\cdot 2H_2O$
Colour		intense-blue	pink	white	orange
Melting point/°C		197	195	202	199
Elemental analysis: found (calcd.)/%	metal	9.71 (10.05)	8.80 (9.13)	8.50 (8.82)	6.10 (6.58)
	C	41.45 (41.81)	40.57 (40.94)	42.01 (42.42)	44.58 (44.36)
	H	3.72 (3.83)	3.79 (3.75)	3.80 (3.88)	4.21 (4.06)
	N	13.04 (13.30)	13.27 (13.02)	13.65 (13.49)	14.27 (14.11)

Thermal measurements were carried out with an OD-103 MOM derivatograph. Sample mass: 100±1÷2 mg, heating rate: 10 K min^{-1}; reference material: Al_2O_3, atmosphere: static air. The infrared spectra were recorded in KBr pellets with a UR-21-spectrophotometer. EPR spectra were recorded at 9.4 GHz (X band), using standard JEOL-JES-3B equipment. Magnetic susceptibility measurements were made on powdered samples with a Faraday balance.

Results and discussion

The thermal behaviour of the ligand and of the synthesized complexes is described in Table 2. Thermal stability domains, melting points, decomposition phenomena (followed as endo and exo effects in the DTA curves and as mass losses, calculated from the TG and DTG curves) and their assignments are presented.

Table 2 Thermal data on γ-*L*-glutamyl-5-(*p*-nitroanilide) and its metal derivatives

Compound	Temperature range/°C	DTA peak/°C		TG mass loss/%	
		endo	exo	calc.	exp.
$L\cdot H_2O$	20–200	115	–	6.31	6.06
		186	–	–	–
	200–400	–	201	16.14	16.22
				31.93	31.65
	400–500	–	420	45.62	45.77
$CuL_2\cdot 2H_2O$	20–200	112	–	5.70	6.18
		197	–	–	–
	200–400	–	200	14.56	43.10
		–	243	28.79	28.48
	400–500	–	450	39.87	41.23
$CoL_2\cdot 3H_2O$	20–200	105	–	2.79	2.76
		130	–	5.58	5.53
		195	–	–	–
	200–400	–	205	14.25	14.12
		–	260	28.23	27.54
		–	430	39.06	38.54
$MnL_2\cdot 2H_2O$	20–200	160	–	5.58	6.31
	200–400	202	–	–	–
		–	206	14.77	14.52
		–	248	29.91	30.28
	400–500	–	438	40.44	38.94
$FeL_3\cdot 2H_2O$	20–200	110	–	4.04	4.21
		198	–	–	–
	200–400	–	202	15.44	15.10
		–	285	30.59	30.89
	400–500	–	460	41.89	41.05

In the temperature range 20–200°C, an endo peak at 115°C in the DTA curve of the ligand indicates the loss of 1 mole of hydrating water. The compound is then stable up to 186°C, where another endo peak indicates its melting point.

Figure 2 presents the DTA, TG and DTG curves recorded on $L\cdot H_2O$ and $FeL_3\cdot 2H_2O$.

The shoulder at ~200°C in the TG, DTG and DTA curves demonstrates that further splitting of the nitroaniline proceeds gradually; according to the literature data, this involves C–NO_2 bond breaking [10]. The first groups lost are the nitro groups, followed by the aniline, corresponding to a net mass loss of 16.22%. This is followed by decomposition, marked by an exo peak at 256°C, corresponding to a net mass loss of 31.65%, due to removal of the organic radical –NH–C_6H_5 obtained from the *p*-nitroaniline used in the *L*-glutamic acid condensation. The theoretical value for the mass loss confirms the proposed assignment. In the temperature range 400–500°C, the remaining *L*-glutamic acid undergoes pyrolysis, as reflected by the exo peak at 420°C.

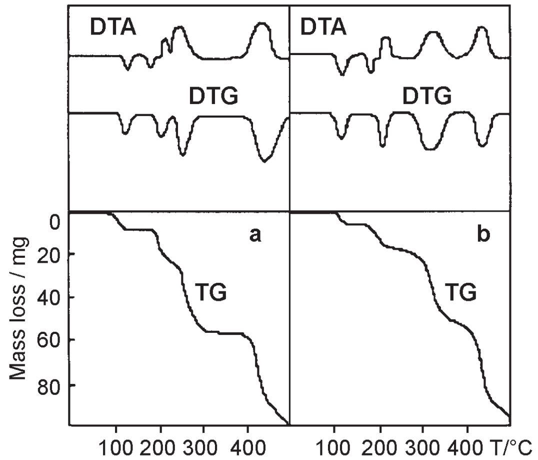

Fig. 2 DTA, TG and DTG curves for a – $L\cdot H_2O$ and b – $FeL_3\cdot 2H_2O$

The peaks at 112 and 110°C, respectively, indicate the endo reactions of $CuL_2\cdot 2H_2O$ and $FeL_3\cdot 2H_2O$, involving the loss of the hydrating water.

Two peaks, at 105 and 130°C, reflect the endo reactions of $CoL_2\cdot 3H_2O$. The mass loss observed in the TG curve indicates the loss of one mole of hydrating water and two moles of coordination water. For this complex, we propose octahedral coordination: $[CoL_2(H_2O)_2]\cdot H_2O$ [11, 12].

The complex $MnL_2\cdot 2H_2O$ undergoes a net mass loss of 6.31% in an endo reaction with a peak at 160°C; this is explained by the loss of two moles of coordination water, leading to an octahedral molecular structure, $[MnL_2(H_2O)_2]$ [11, 12].

The melting points of the complexes lie in the temperature range 195–202°C in the DTA curves. They are associated with endothermic peaks with values higher than that of the ligand, as proof of metal–nitrogen and metal–oxygen bonding formation. The thermal stability of the molecule is increased by complexation.

In the temperature range 400–500°C, pyrolysis occurs and all of the studied compounds lose the *L*-glutamic acid radical. A comparison of the theoretical stoichiometric data on the residual metal oxide, the ligand loss and the crystal water with the experimental data leads to metal ligand:water ratios similar to those obtained on chemical analysis.

Table 3 presents some IR absorption bands and their assignments for the ligand and the metal compounds.

Table 3 Some IR absorption bands (cm^{-1}) for the ligand and its metal complexes

Assignment	$L\cdot H_2O$	$CuL_2\cdot 2H_2O$	$CoL_2\cdot 3H_2O$	$MnL_2\cdot 2H_2O$	$FeL_3\cdot 2H_2O$
ν(O–H); ν(O–H–O)	3500	3525	3560	3510	3534
$\nu(NH_2)$	3280	3180	3152	3125	3100
ν(C=O)	1700	1640	1628	1617	1610
ν(C–O)	1375	1354	1362	1370	1368
$\rho_t(NH_2)$	1244	1216	1225	1230	1226
$\rho_w(NH_2)$	1020	1056	1026	1038	1028
$\nu(M–OH_2)$	–	–	762	760	–
δ(C=O)	744	725	730	732	735
π(C=O)	620	612	592	590	602
ν(M–N)	–	446	440	438	435

A comparative study of these spectral data reveals the lowering of the ν(C=O) frequency values from 1700 for the ligand to 1610–1640 cm^{-1} for the complexes, indicating the involvement of the carbonyl oxygen atom in the metal coordination [13].

The shifts in the $\nu(NH_2)$ vibration bands indicate the involvement of the nitrogen atom from the secondary amino group in the metal coordination.

Due to the increased number of hydrogen-bonds, the ν(O–H–O) vibration band is slightly shifted for the complexes.

The additional bands at 760 and 762 cm^{-1} in the IR spectra of $CoL_2\cdot 4H_2O$ and $MnL_2\cdot 2H_2O$ are characteristic of water molecules in the inner coordination sphere [14, 15].

The ν(C=O) and $\nu(NH_2)$ stretching vibrations are shifted to lower frequencies in the sequence Fe(III)<Mn(II)<Co(II)<Cu(II). The IR data are in good agreement with the Irving–Williams stability series [16, 17].

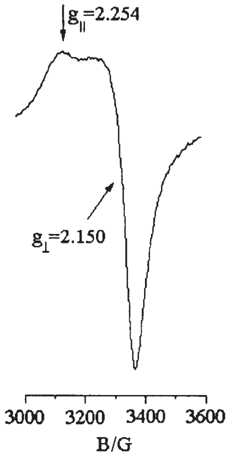

Fig. 3 Powder spectrum of $CuL_2\cdot 2H_2O$ at room temperature

The powder ESR spectrum of $CuL_2{\cdot}3H_2O$ at room temperature (Fig. 3) is typical of pseudotetrahedral monomeric species. The values $g_{||}$=2.254 and $g_{\perp}$=2.150 correspond to a CuN_2O_2 chromophore [18].

The powder ESR spectrum of $MnL_2{\cdot}2H_2O$ is characterized by a quasi-isotropic *g* tensor with principal value (*g*=2.0018) close to the spin-only value.

The ESR spectrum of $FeL_3{\cdot}2H_2O$ is almost isotropic (*g*=2.002). The presence of a weak signal at *g*≈4 suggests a small distortion of the octahedral symmetry around the metal ion.

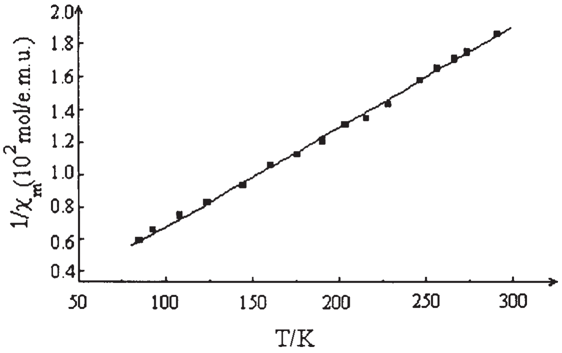

Fig. 4 Temperature dependence of $1/\chi_m$ for $CoL_2{\cdot}3H_2O$

The magnetic susceptibility measurements indicate Curie-Weiss behaviour (Fig. 4), with magnetic moments specific for monomeric species. The value obtained for the magnetic moment of the Cu(II) complex (μ_{eff}=1.71μ_B) is in the range normally observed for pseudotetrahedral species, while those corresponding to high-spin Co(II), Mn(II) and Fe(III) (μ_{eff}=3.627μ_B, 6.71μ_B and 5.05μ_B, respectively) rather suggest local octahedral environments. The paramagnetic Curie temperatures (θ=5–12 and 35 K for the Cu(II), Co(II) and Fe(III) complexes, respectively) indicate the presence of exchange interactions between the metal ions, due to the formation of intermolecular hydrogen-bonds [19].

Conclusions

The thermal and spectroscopic behaviour of the synthesized metal complexes indicates that their stability sequence:

$$CuL_2{\cdot}2H_2O>CoL_2{\cdot}4H_2O>MnL_2{\cdot}4H_2O>FeL_3{\cdot}5H_2O$$

conforms with the Irving-Williams series [15, 16].

The IR spectra demonstrate that γ-*L*-glutamyl-5-(*p*-nitroanilide) acts as a bidentate ligand, its coordination involving the carbonyl oxygen and the nitrogen atom of the second amino group. For the intermediate class Lewis acids Co(II) and Mn(II), two H_2O molecules are involved in the metal ion coordination, resulting in an octahedral local structure. Three bidentate ligand molecules are coordinated to the class '*a*' Lewis acid Fe(III). The ESR spectra and magnetic data confirm pseudo-tetrahedral (for the Cu(II) ion) and octahedral (for the Co(II), Mn(II) and Fe(III) ions) local symmetries.

The structural data obtained allow proposal of the following molecular formulae for the studied metal complexes:

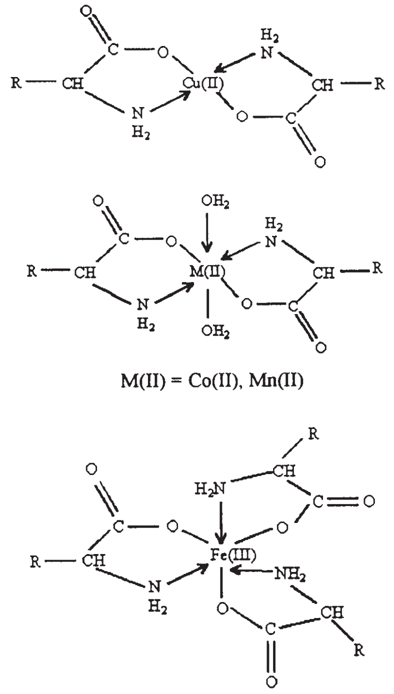

M(II) = Co(II), Mn(II)

Fig. 5 Suggested structures of the studied complexes (R=$C_6H_5O_2N_2$)

References

1 J. Charlson, K. E. Trainer and E. C. Walton, J. Proc. R. Soc. N. S. W., 108 (1975) 1.

2 L. F. Mackenzie, G. J. Davies, M. Schuelein and S. G. Withers, Biochemistry, 36 (1997) 5893.

3 A. Adach, J. Janyst and M. Cieslak-Golonka, Spectrosc. Lett., 28 (1995) 1259.

4 P. Francesco, J. Chromatogr.A, 802 (1998) 315.

5 K. J. Alok and K. Farid, J. Electrochem. Soc. India, 45 (1996) 115.

6 M. Orlowski, Arch. Immun. Therapie, 13 (1965) 538.

7 Ye. I. Dudina, V. Ye. Formazyuk, V. I. Sergiyenko and T. N. Gorshkhova, Vestn. Ross. Akad. Med. Nauk, 3 (1995) 31.

8 F. Tellier, F. Acher, I. Brabet, J. P. Pin, J. Bockaert and R. Azerad, C. R. Acad. Sci. Ser. II, Mec. Phys., Chim. Astron., 321 (1995) 385.

9 M. Simihăian, S. Kiss, D. Paşca and C. Suciu, Studia Univ. Babeş-Bolyai, Biologia, 37 (1992) 99.

10 K. Raha, P. S. Makashir and E. W. Kusian, J. Thermal Anal., 35 (1989) 1173.

11 P. G. Olafsson and A. M. Bryan, Microchim. Acta, (1970) 871.
12 S. L. Stefan, J. Thermal Anal., 42 (1994) 1299.
13 K. Nakamoto, 'Infrared Spectra of Inorganic and Coordination Compounds', Wiley, New York 1970.
14 S. L. Stefan, B. A. El-Shetary, W. G. Hanna and S. B. El-Maraghy, Microchemical J., 35 (1987) 51.
15 H. A. Dessouky, R. M. Issa and M. M. Moustafa, Acta Chim. Hung., 126 (1969) 653.
16 J. J. R. Frausto da Silva and R. J. P. Williams, 'The Biological Chemistry of the Elements', Clarendon Press, Oxford 1994.
17 W. B. Jensen, 'The Lewis Acid-base Concepts', Wiley, New York 1980.
18 F. E. Mabbs and D. Colisson, 'Electron Paramagnetic Resonance of d Transition Metal Compounds', Elsevier, Amsterdam 1992.
19 R. L. Carlin, 'Magnetochemistry', Springer Verlag, Berlin 1986.